University of Groningen

N-Ras induces alterations in Golgi complex architecture and in constitutive protein transport

Babia, Teresa; Ayala, Inmaculada; Valderrama, Ferran; Mato, Eugènia; Bosch, Marta; Santarén, Juan F. ; Renau-Piqueras, Jaime; Kok, Jan Willem; Thomsen, Timothy M.; Egea, Gustavo

Published in:
Journal of Cell Science

IMPORTANT NOTE: You are advised to consult the publisher's version (publisher's PDF) if you wish to cite from it. Please check the document version below.

Document Version
Publisher's PDF, also known as Version of record

Publication date:
1999

Link to publication in University of Groningen/UMCG research database

Citation for published version (APA):
Babia, T., Ayala, I., Valderrama, F., Mato, E., Bosch, M., Santarén, J. F., Renau-Piqueras, J., Kok, J. W., Thomsen, T. M., & Egea, G. (1999). N-Ras induces alterations in Golgi complex architecture and in constitutive protein transport. *Journal of Cell Science*, *112*(4), 477-489. http://jcs.biologists.org/content/112/4/477.long

Copyright
Other than for strictly personal use, it is not permitted to download or to forward/distribute the text or part of it without the consent of the author(s) and/or copyright holder(s), unless the work is under an open content license (like Creative Commons).

The publication may also be distributed here under the terms of Article 25fa of the Dutch Copyright Act, indicated by the "Taverne" license. More information can be found on the University of Groningen website: https://www.rug.nl/library/open-access/self-archiving-pure/taverne-amendment.

Take-down policy
If you believe that this document breaches copyright please contact us providing details, and we will remove access to the work immediately and investigate your claim.

Downloaded from the University of Groningen/UMCG research database (Pure): http://www.rug.nl/research/portal. For technical reasons the number of authors shown on this cover page is limited to 10 maximum.

Journal of Cell Science 112, 477-489 (1999)
Printed in Great Britain © The Company of Biologists Limited 1999
JCS7330

N-Ras induces alterations in Golgi complex architecture and in constitutive protein transport

Teresa Babià[1], Inmaculada Ayala[1], Ferran Valderrama[1], Eugènia Mato[1,2], Marta Bosch[1], Juan F. Santarén[3], Jaime Renau-Piqueras[4], Jan Willem Kok[5], Timothy M. Thomson[6] and Gustavo Egea[1,*]

[1]Departament de Biologia Cel.lular, Facultat de Medicina, IDIBAPS, Universitat de Barcelona, C/Casanova, 08036 Barcelona (Spain)
[2]Servei d'Endocrinologia, Hospital de Sant Pau, Barcelona, Spain
[3]Centro de Biología Molecular Severo Ochoa (CBMSO), UAM-CSIC, Madrid, Spain
[4]Centro de Investigación, Hospital La Fe, València, Spain
[5]Department of Physiological Chemistry, University of Groningen Medical School, Groningen, The Netherlands
[6]Centre d'Investigació i Desenvolupament, CSIC, and Centre d'Investigació en Bioquímica i Biologia Molecular, Hospitals Vall d'Hebron, Barcelona, Spain
*Author for correspondence (e-mail: egea@medicina.ub.es)

Accepted 1 December 1998; published on WWW 25 January 1999

SUMMARY

Aberrant glycosylation of proteins and lipids is a common feature of many tumor cell types, and is often accompanied by alterations in membrane traffic and an anomalous localization of Golgi-resident proteins and glycans. These observations suggest that the Golgi complex is a key organelle for at least some of the functional changes associated with malignant transformation. To gain insight into this possibility, we have analyzed changes in the structure and function of the Golgi complex induced by the conditional expression of the transforming N-Ras(K61) mutant in the NRK cell line. A remarkable and specific effect associated with this N-Ras-induced transformation was a conspicuous rearrangement of the Golgi complex into a collapsed morphology. Ultrastructural and stereological analyses demonstrated that the Golgi complex was extensively fragmented. The collapse of the Golgi complex was also accompanied by a disruption of the actin cytoskeleton. Functionally, N-Ras-transformed KT8 cells showed an increase in the constitutive protein transport from the trans-Golgi network to the cell surface, and did not induce the appearance of aberrant cell surface glycans. The Golgi complex collapse, the actin disassembly, and the increased constitutive secretion were all partially inhibited by the phospholipase A_2 inhibitor 4-bromophenylacyl bromide. The results thus suggest the involvement of the actin cytoskeleton in the shape of the Golgi complex, and intracellular phospholipase A_2 in its architecture and secretory function.

Key words: Ras, Golgi complex, Secretory pathway, Actin, Phospholipase A_2

INTRODUCTION

The Ras-related small GTPases are key regulators of several biological phenomena (Bourne et al., 1990; Hall, 1990), including vesicular traffic (Rab, Arf and Sar; Pfeffer, 1994) and the dynamics of the actin cytoskeleton (Rho; Symons, 1996; Machesky and Hall, 1996). Ras mutations are frequently involved in experimental and spontaneously occurring tumors (Bos, 1989), which means it is particularly relevant to study its contribution to changes in organelle interaction and functions brought about by transformation. Previous studies have shown that the oncogenic Ras proteins induce numerous alterations in processes that affect cellular structure and organization, such as cytoskeletal reorganization (Bar-Sagi and Feramisco, 1986; Dartsch et al., 1994), pinocytosis (Bar-Sagi and Feramisco, 1986), cell swelling (Lang et al., 1992), alterations in the calcium metabolism (Wöll et al., 1992) and changes in cell surface glycosylation (Santer et al., 1984; Collard et al., 1985; Bolscher et al., 1986, 1988). Malignant transformation is frequently accompanied by aberrant glycosylation of proteins and lipids, which could contribute to certain properties of transformed cells, such as abnormal adhesion to the extracellular matrix or to other cells, with consequences as to their invasive and metastasic potential (Hakomori, 1989; Dennis, 1991).

The Golgi complex (GC) plays an important role in post-translational modifications and sorting of lipids and proteins transported from the endoplasmic reticulum (ER). A distinctive feature of the GC is the hierarchical compartmentalization of its components and their arrangement in a functional order, which introduces a variety of post-translational modifications into the lipids and proteins transported through the organelle (Berger and Roth, 1997; Farquhar and Palade, 1998). Recently, extensive evidence that the GC could also be a target for

signalling molecules has emerged, since some have been immunolocalized in the organelle and/or functionally shown to be directly involved in vesicular transport. Examples include 14-3-3 proteins (Gelperin et al., 1995), phospholipase A (Morreau and Morre, 1991; Slomiany et al., 1992; Tagaya et al., 1993), phospholipase D (Ktistakis et al., 1995), several protein kinase C isoenzymes (De Matteis et al., 1993; Goodnight et al., 1995; Prestle et al., 1996; Simon et al., 1996; Buccione et al., 1996), protein kinase A (Pimplikar and Simons, 1994; Muñiz et al., 1996), the MAP kinase ERK (Acharya et al., 1998), and heterotrimeric G-protein subunits (Melançon et al., 1987; Stow et al., 1991; Bomsel and Mostov, 1992; Leyte et al., 1992; Denker et al., 1996).

To establish direct links between cell transformation induced by a single oncogene, alterations in membrane trafficking, the structure and function of the GC, and the appearance of aberrant glycosylation, we have developed and characterized a cellular model (KT8 cell line) for the conditional expression of the murine N-*ras* oncogene. In N-Ras-transformed KT8 cells, the GC is collapsed and fragmented, the actin cytoskeleton is disrupted, and an increase in the constitutive protein transport from the trans-Golgi network (TGN) to the cell surface is observed. Moreover, these alterations were partially prevented by the inhibiton of intracellular phospholipase A_2 (PLA_2), suggesting its involvement in the secretory pathway.

MATERIALS AND METHODS

Cell transfection

Normal rat kidney (NRK) 44F cells (American Type Culture Collection, Rockwell, MD, USA) were co-transfected by the calcium phosphate method with the plasmid pMMTV-N-ras^T containing the transforming mouse N-*ras* gene (Lys 61) under the transcriptional control of the glucocorticoid-inducible MMTV LTR (Guerrero et al., 1986), and the plasmid pIBW3neo (Bond and Wold, 1987), for the expression of the neomycin resistance gene. Stable transfectants were selected by resistance to 400 μg/ml geneticin (Sigma, St Louis, MO, USA). After expansion of the clones, transfected cells were routinely maintained in culture medium containing 200 μg/ml geneticin.

Single-stranded conformational polymorphism

RNA was extracted by the guanidinium isothiocyanate method (Chomczynski and Sacchi, 1987), and 1 μg of RNA was used for reverse transcription in 2.5 mM $MgCl_2$, 10 mM Tris-HCl, pH 8.3, 50 mM KCl, 39 units/μl RNAguard (Pharmacia, Uppsala, Sweden), 200 units/μl Mo-MuLV-reverse transcriptase (BRL Gibco, UK), 200 μM deoxynucleoside triphosphates, and random hexamers, at 42°C for 30 minutes. 5 μl of this reaction were used in polymerase chain reactions (PCR) by using 1 μM of the primers that correspond to exons 1 and 2 of murine N-*ras* (TGACTGAGTACAAACTGG and CTGTAGAGGTTAATATCT). 5 μl of the PCR product were diluted (1:16) in 95% formamide, 10 mM EDTA, 0.05% Bromophenol Blue, 0.05% xylene cyanol, and incubated at 95°C for 3 minutes. Samples were ice-cooled and loaded onto a 12% sodium dodecyl sulfate (SDS) polyacrylamide gel, and electrophoresed at room temperature for 12-15 hours at 5 W. Subsequently, gels were fixed, silver-stained and dried.

Western blotting

Cells were lysed in 80 mM Tris-HCl, pH 6.5, 0.5% SDS. Protein samples from lysates (30-60 μg/sample) were electrophoresed by 10% or 15% SDS-PAGE, and the gels were transferred onto Immobilon-P membranes (Millipore Corporation, Bedford, MA, USA). The Immobilon-P sheets were preincubated in TBS buffer (20 mM Tris-HCl, pH 7.5, 150 mM NaCl) with 5% defatted milk powder for 1 hour at room temperature, followed by incubation with 5 μg/ml of affinity-purified mouse monoclonal IgG antibody to the amino-terminal domain of $cPLA_2$ (Santa Cruz Biotechnology, Santa Cruz, CA, USA) or 10 μg/ml of mouse monoclonal anti-pan-Ras (Ab-2) antibody (Oncogene Sciences, Uniondale, NY, USA) in TBS with 1% bovine serum albumin (BSA) and 0.5% defatted milk powder for 1 hour. Blots were rinsed three times in TBST (TBS buffer containing 0.05% Tween 20). Subsequently, strips were incubated with alkaline phosphatase-conjugated anti-mouse IgG antibody (1:10,000) (Promega Corporation, Madison, WI, USA) for 1 hour. After three rinses in TBST and one in TBS, the reaction was visualized with NBT/BCIP.

Immunofluorescence

Cells were grown on coverslips to 70-90% confluency, quickly washed in PBS (10 mM phosphate buffer, 150 mM NaCl, pH 7.2) and fixed either by immersion in cold (–20°C) methanol for 2-3 minutes or in freshly prepared paraformaldehyde (4% in PBS) at room temperature for 15 minutes. Subsequently, coverslips were washed in PBS and, in the case of paraformaldehyde fixation, free aldehyde groups were blocked by incubation with 50 mM NH_4Cl in PBS for 30 minutes. Thereafter, cells were permeabilized for 15 minutes with PBS containing 0.1% saponin and 1% BSA and further processed for single- or double-label immunofluorescence as previously described (Alcalde et al., 1994) using the following dilutions of the primary antibodies: rabbit anti-Man II (1:4,000) (Dr A. Velasco, University of Sevilla, Spain), rabbit anti-PDI (1:100) (Dr J.G. Castaño, Universidad Autónoma de Madrid, Spain), mouse monoclonal E3A5 (1:20) (Sigma Co., St Louis, MO, USA), rabbit anti-β-COP (1:60) (Dr T. Kreis, University of Geneva, Switzerland), rabbit anti-ERK2 (1:100) (Upstate Biotechnology Inc, Lake Placid, NY, USA), rabbit anti-VSV glycoprotein ectocytoplasmic domain (1:300) (Dr K. Simons, EMBL, Heidelberg, Germany), mouse monoclonal P5D4 anti-VSV glycoprotein carboxy-terminal amino acids (497-511) (1:800) (Sigma Co., St Louis, MO, USA), mouse monoclonal anti-actin (1:400) (ICN, Costa Mesa, CA, USA) and anti-β-tubulin (1:200) (Boehringer Mannheim, Mannheim, Germany), and TRITC- or FITC-phalloidin (1:250 from a stock solution of 0.2 mg/ml; Sigma Co., St Louis, MO, USA). Polyclonal or monoclonal antibodies were visualized with TRITC- or FITC-conjugated anti-rabbit IgG $F(ab')_2$ or anti-mouse IgG $F(ab')_2$ fragments (1:30) (Boehringer Mannheim, Mannheim, Germany). Samples were viewed either under an Olympus BX60 fluorescent microscope or under a Leica TCS 4D confocal microscope.

Electron microscopy and stereological analyses

Cells were washed twice in 100 mM cacodylate buffer (pH 7.2) and fixed with 2.5% glutaraldehyde in this buffer for 60 minutes at room temperature. Cells were then washed (3×, 5 minutes each) with 100 mM cacodylate buffer and post-fixed with 1% (v/v) OsO_4/1.5% (w/v) $K_4Fe(CN)_6$ in 100 mM cacodylate buffer for 1 hour at 4°C. Cells were scraped, pelleted and treated for 1 hour at 4°C with 1% tannic acid in cacodylate buffer, rinsed in distilled water, and stained en bloc with 1% aqueous uranyl acetate for 1 hour, followed by dehydration through graded ethanols and embedding in Epon 812. Ultrathin sections were stained with lead citrate for 2 minutes and observed in a Philips 301 electron microscope.

Randomly selected micrographs were taken at the same magnification (×47,500, final magnification) and analyzed using point-counting procedures (Weibel, 1979). The GC was defined as a group of cisternae organized in stacks with tubular and vesicular structures. Total GC (tGC) was defined as an area containing at least one cisterna and Golgi vesicles, with an arbitrary border in the cytoplasm surrounding the GC (Renau-Piqueras et al., 1987). Intermediate elements in continuity with the rough ER were excluded.

The following stereological parameters were determined using standard procedures (Weibel, 1979; Renau-Piqueras et al., 1987): the volume density (V_{vi}) of the tGC relative to the cytoplasm (V_{vi} tGC/cytopl); the V_{vi} of cisternae relative to the cytoplasm (V_{vi} cist/cytopl); the V_{vi} of cisternae relative to the tGC (V_{vi} cist/tGC); the surface density (S_{vi}) of cisternae relative to the cytoplasm (S_{vi} cist/cytopl); and the S_{vi} of cisternae relative to the tGC (S_{vi} cist/tGC). The minimum sample size (number of micrographs) of each stereological parameter was determined by the progressive mean technique (confidence limit ≤5%) (Williams, 1977). The results, expressed as means ± s.d., were compared using the Student's *t*-test.

Virus infection, VSV-G protein two-dimensional gel electrophoresis and VSV-G protein transport assays

Cell monolayers were infected at 25 p.f.u./cell with the vesicular stomatitis virus (VSV) temperature-sensitive mutant ts045 virus in Dulbelcco's modified essential medium (DMEM; BRL Gibco, UK) without fetal calf serum (FCS) at 32°C. At 4 hours post-infection in DMEM containing 10% FCS, Pro-Mix L-[^{35}S]cell-labeling mix (Amersham, Buckinghamshire, UK) was added in methionine/cysteine-free DMEM (ICN, Costa Mesa, CA, USA).

For continuous metabolic labeling, infected cells were incubated for 2 hours at 32°C in the presence of 1 mCi/ml of Pro-Mix L-[^{35}S]. Labeled cells were washed with cold culture medium containing 2 mM methionine and cysteine, lysed in 100 μl Triton X-100 lysis buffer (1% Triton X-100, 50 mM Tris-HCl, pH 8.0, 62.5 mM EDTA) at 4°C for 30 minutes, and centrifuged at 14,000 ***g*** for 15 minutes. To supernatants were added 200 μl detergent solution (62.5 mM EDTA, 50 mM Tris-HCl, pH 8.0, 0.4% sodium deoxycholate, DOC, 1% Nonidet P40, NP40), 8 μl 10% SDS and 2 μl mouse monoclonal P5D4 anti-VSV-G protein antibody, followed by an overnight incubation at 4°C. Then, samples were incubated with rabbit-anti mouse IgG (Dako, Denmark) for 1 hour at 4°C, followed by 20 μl of protein A/G agarose (Sta Cruz Biotechnology, Inc., Sta Cruz, CA, USA) for 45 minutes at room temperature; subsequently, samples were washed 3× in RIPA buffer (10 mM Tris-HCl, pH 7.4, 0.1% SDS, 1% DOC, 1% NP40, 150 mM NaCl), 3× in TENEN high salt buffer (10 mM Tris-HCl, pH 7.2, 500 mM NaCl, 1 mM EDTA, 0.5% NP40, 0.1% SDS), and once in PBS. Pellets were resuspended in electrophoresis sample buffer, boiled for 5 minutes, and processed for two-dimensional gel electrophoresis. Gels were processed for fluorography, dried and exposed at –80°C. Quantitation of radioactive proteins was performed as previously described (Santarén and García-Bellido, 1990).

For pulse-chase metabolic labeling experiments, VSV ts045 virus-infected cells were incubated for 15 minutes in methionine-free DMEM at 40°C and pulse-labeled in suspension for 10 minutes with 100 μCi/ml Pro-Mix L-[^{35}S]cell-labeling mix at 40°C. Cells were washed with ice-cold PBS and chased at 32°C in methionine-containing medium for the indicated times. After the chase, cells were washed twice with ice-cold PBS and lysed for 15 minutes on ice with Triton X-100 lysis buffer. Immunoprecipitation was carried out as described above, except that after the last PBS rinse, the protein A/G agarose beads were resuspended in 10 μl of BH1 buffer (100 mM sodium acetate, pH 5.5, 1% SDS, 0.1% Triton X-100) and proteins were eluted from the beads by heating at 95°C for 5 minutes. The supernatant was recovered by centrifugation and 30 μl BH2 buffer (100 mM sodium acetate, pH 5.5, 1 mM PMSF, 5 μg/ml aprotinin, 1 mM benzamidin) was added. Subsequently, 0.25 mi.u. of Endo H (Boehringer Mannheim, Mannheim, Germany) was added, and the samples were incubated overnight at 37°C. They were then separated under reducing conditions by 7.5% SDS-PAGE, and gels were fluorographed. Band quantitation was performed with the Phoretix image analysis software (Phoretix International Ltd, Newcastle, England).

For cell surface biotinylation, cells were plated at confluence, infected and pulse-labeled as described above, except that the virus adsorption was performed in the presence of 5 μg/ml actinomycin D (Buccione et al., 1996). After the pulse at the non-permissive temperature, cells were either immediately placed on ice, or chased at 37°C in the presence of DMEM containing 5% FCS and 2 mM methionine for the indicated periods of time. Cell surface proteins were biotinylated according to de Hoop and Cid-Arregui (1996): cells were washed twice with PBS$^+$ (PBS containing 0.1 mM $CaCl_2$ and 0.1 mM $MgCl_2$) and surface biotinylated by incubating for 30 minutes with 0.5 ml NHS-LC-biotin (1 mg/ml; Pierce, Rockford, IL, USA) in PBS$^+$ on ice. Then, cells were washed twice with PBS$^+$, quenched (2×, 5 minutes each) with PBS$^+$ containing 100 mM glycine and 0.3% bovine serum albumin (BSA), and washed twice in PBS$^+$. Biotinylated cells were lysed for 10 minutes on ice in lysis buffer (2% NP-40, 0.2% SDS in PBS supplemented with protease inhibitors). Lysates were centrifuged at 14,000 ***g*** at 4°C, and samples of the supernatant were precipitated with trichloroacetic acid or incubated overnight at 4°C by rotation with streptavidin-agarose (Pierce, Rockford, IL, USA). The beads were centrifuged at 14,000 ***g*** for 30 seconds and washed in RIPA and TENEN high salt buffers. Bound material was eluted with 30 μl of 1× SDS sample loading buffer, and analysed by 7.5% acrylamide SDS-PAGE. Finally, gels were dried, fluorographed and VSV-G protein bands quantitated by both Phoretix Image analysis and scintillation counting.

Release of secretory proteins

Cell monolayers were pulse labeled with 100 μCi/ml Pro-Mix L-[^{35}S]cell-labeling mix for 5 minutes at 37°C in pulse medium, washed three times with cold culture medium containing 2 mM methionine, and incubated at 37°C for the indicated times. Then, the cell culture medium was collected, and centrifuged at 14,000 ***g*** for 30 minutes, and the supernatants were precipitated with trichloroacetic acid, resuspended in 1× sample buffer, eluted and analyzed by SDS-PAGE. Parallel samples were quantitated by scintillation counting.

Fluorescent phalloidin-binding assay

Cell cultures were fixed in 4% paraformaldehyde in PBS for 15-30 minutes and permeabilized with 0.1% Triton X-100 in PBS for 5 minutes. After 3 rinses in PBS, cells were incubated with TRITC-phalloidin (1:1,000 from a stock solution of 0.2 mg/ml) in PBS for 15 minutes, washed 3 times in PBS, and extracted with methanol for 25 minutes at room temperature. The fluorescence intensity of the supernatants was quantified in a Kontron Instruments fluorimeter (SFM25) with 554 nm and 573 nm excitation and emission wavelengths, respectively.

Lectin-mediated cytotoxicity assay

Cells were plated in each well of a 24-well plate (2×10^5/well) in 0.5 ml DMEM containing 5% FCS and incubated overnight at 37°C. Increasing concentrations of wheat germ agglutinin (WGA) and L-phytohemagglutinin (L-PHA) (Sigma Co, St Louis, MO, USA) were added to the cells, followed by an incubation at 37°C until the cells containing no lectin grew to confluence. The medium was removed, and the cells were rinsed in PBS without Ca^{2+} and Mg^{2+}, trypsinized, centrifuged and counted. The results were expressed as the survival percentage of cells for each lectin concentration.

Cytosolic phospholipase A_2 activity assay

Calcium-dependent cytosolic phospholipase A_2 (cPLA$_2$) activity was measured using a colorimetric assay (Alexis Corporation, Läufelfingen, Switzerland). Briefly, cells were lysed with Triton X-100 lysis buffer and centrifuged at 14,000 ***g*** for 15 minutes at 4°C. Lysates were concentrated with Centricon centrifuge concentrators (Amicon Inc., Beverly, MA, USA) with a molecular mass cut-off of 30 kDa to remove any residual secretory PLA$_2$ (sPLA$_2$). Bromoenol lactone was added to the lysates to inhibit any calcium-independent cytosolic PLA$_2$ (iPLA$_2$). Equal final volumes and sample protein contents were placed into ELISA wells, and the reaction was performed according to the manufacturer's instructions. A positive

control (bee venom PLA_2) was also included each time. The reaction product was revealed with Ellman's reagent (DTNB) and quantitated by reading the absorbance at 405 nm using an ELISA plate reader. Results are expressed as nmol/minute/ml.

RESULTS

NRK cells were stably transfected with the mouse N-*ras* gene (Guerrero et al., 1986) under the transcriptional control of the glucocorticoid inducible MMTV LTR promotor. A cell line, designated KT8, was generated and used for the present study. Analysis by RT-PCR and SSCP of the expression of oncogenic mouse N-*ras* in KT8 cells demonstrated that two types of N-*ras* gene transcripts were expressed after incubation with dexamethasone, corresponding to the endogenous, wild-type N-*ras*, and to the exogenous, mutated N-*ras* genes (Fig. 1A). The oncogenic N-Ras protein [N-Ras(K61)] was visualized by immunoblotting after 8-12 hours of exposure to various concentrations of dexamethasone (Fig. 1B). Expression of the exogenous gene and proteins was accompanied with a translocation of the MAP kinase ERK2 into the nucleus and to the plasma membrane (Fig. 1D) (Chen et al., 1992; González et al., 1993). Concomitantly, induced KT8 cells acquired a morphology characteristic of transformed fibroblasts (Fig. 2). These features were maintained for as long as the inducer was present in the culture medium.

N-Ras alters the morphology and the cytological positioning of the Golgi complex

We first studied the effect of N-Ras-induced transformation on the structure and function of the GC. Using antibodies against mannosidase II (Man II), the GC of control NRK and KT8 cells showed a characteristic perinuclear distribution with an interconnected reticular morphology (Fig. 3A,C). Dexamethasone-induced KT8 cells (Fig. 3D), but not dexamethasone-treated NRK cells (Fig. 3B), showed a striking change in this arrangement into a morphological collapse in a juxtanuclear positioning. Similar images were observed when the GC was stained with antibodies against the coatomer

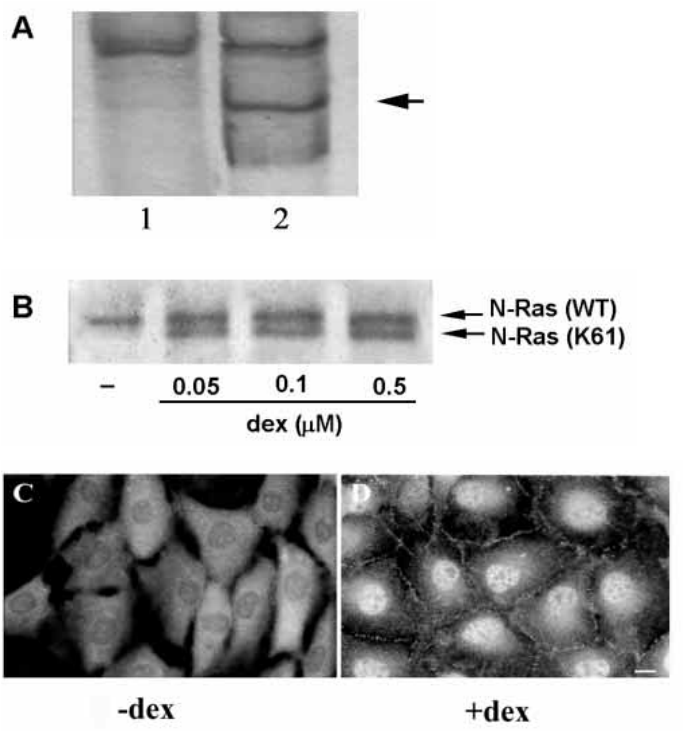

Fig. 1. KT8, a cell line derived from NRK fibroblasts undergoing conditional transformation by N-Ras(K61). (A) Dexamethasone-induced expression of murine N-*ras* oncogene in KT8 cells. RT-PCR/SSCP analysis showing induction of the mutated murine N-*ras* RNA (arrow) after 6 hours in the presence of dexamethasone (0.5 μM; lane 2) compared to non-treated cells (lane 1). (B) Induction of N-Ras(K61) protein in KT8 cells. Cells incubated for 12 hours with different concentrations of dexamethasone (dex) were analyzed for the expression of Ras proteins by western blotting. Note the appearance of wild type (WT) and mutated [NRas(K61)] N-Ras proteins. The latter is seen as a band with faster electrophoretic mobility only in the presence of dexamethasone. (C,D) Translocation of ERK2 in induced KT8 cells. Indirect immunofluorescence microscopy showing ERK2 in control (C) and in dexamethasone-induced (12 hours) KT8 cells (D). Note that ERK2 is translocated both to the nucleus and the plasma membrane in dexamethasone-induced KT8 cells.

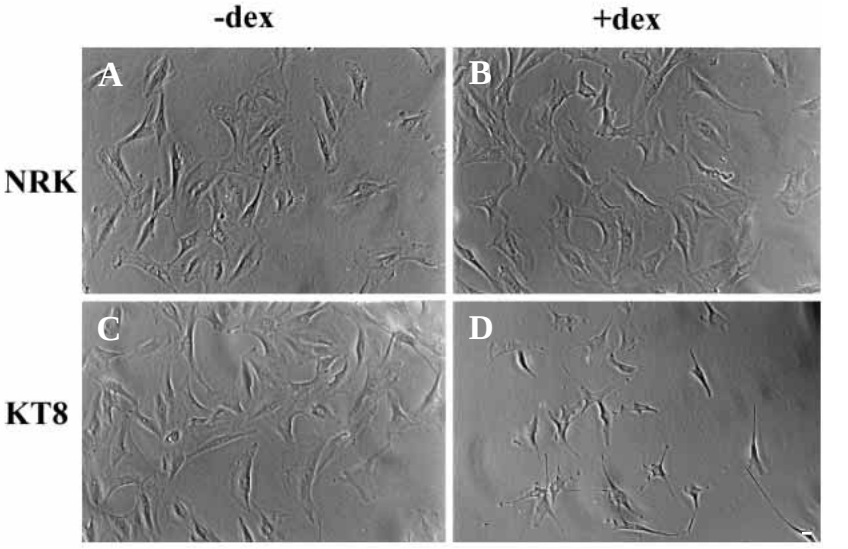

Fig. 2. Morphological transformation of KT8 cells by oncogenic N-*ras* expression. NRK (A,B) and KT8 (C,D) cells were incubated (16 hours) in the presence of ethanol (0.1%) (A,C) or dexamethasone (0.5 μM) (B,D). Note the appearance of long processes and a transformed morphology only in dexamethasone-induced KT8 cells. Bar, 10 μm.

Table 1. Stereological analysis of the GC in control and N-Ras(K61)-transformed cells

	V_{vi}t GC/cytopl	V_{vi} cist/cytopl	V_{vi} cist/tGC	S_{vi} cist/cytopl	S_{vi} cist/tGC
Control cells (*N*=11)	12.57±3.55	5.02±1.82	43.57±9.08	1.23±0.45	11.07±3.43
Induced cells (*N*=11)	12.81±3.68	5.09±1.88	42.79±10.32	1.75±0.31*	15.39±4.09*

*Significant differences with respect to control; Student's *t*-test ($P \leq 0.05$).
V_{vi} = volume density expressed as %.
S_{vi} = surface density expressed as μm^{-1} (area surface of cisternae/volume cytoplasm).
Parameters are defined in Materials and Methods.

component β-COP (Fig. 3F), or the trans-Golgi network (TGN) marker TGN-38, or with the vital Golgi marker NBD-ceramide (not shown). This change in the morphology and cytological positioning of the GC was observed in the majority of the KT8 cells after 12-16 hours of induction with dexamethasone, and was stable for at least 64 hours of continued exposure to the inducer. The GC collapse reverted to its normal morphology and arrangement after removal of the inducer from the culture medium (Fig. 8 and see below). On the other hand, control and dexamethasone-induced KT8 cells stained with antibodies against the ER protein marker PDI (protein disulphide isomerase) showed no difference in the ER staining pattern (Fig. 3G,H).

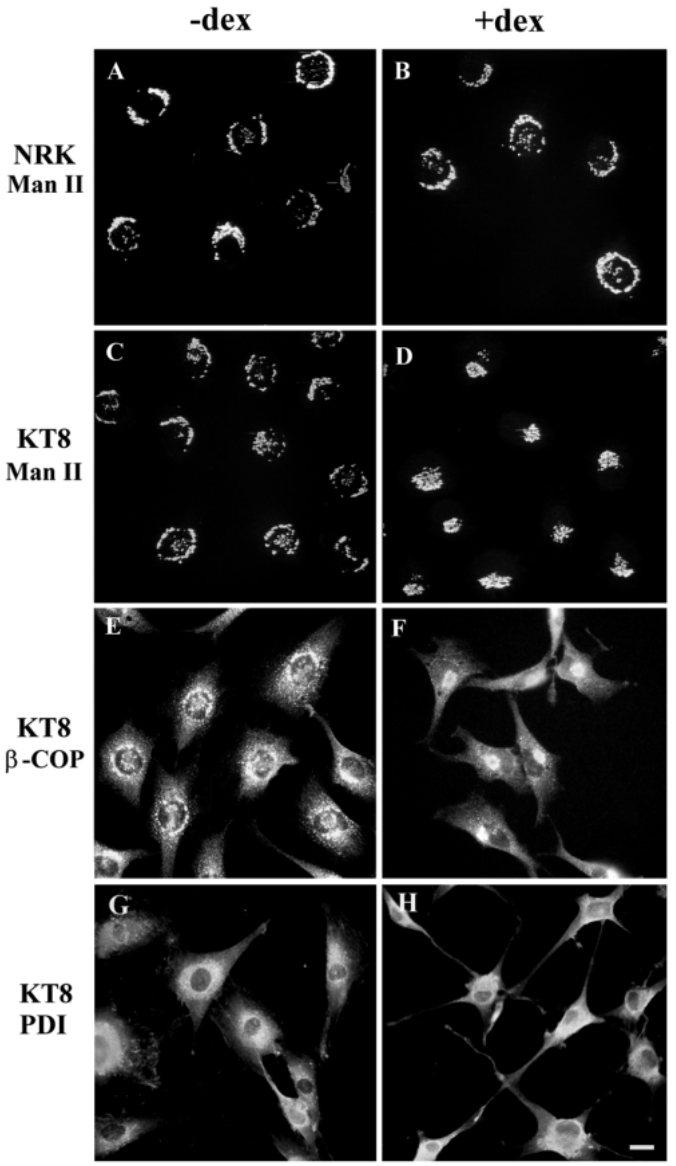

Fig. 3. Morphological collapse of the Golgi complex in N-Ras-transformed KT8 cells. NRK (A,B) and KT8 (C-F) cells were incubated for 16 hours in the presence of solvent alone (0.1% ethanol) (A,C,E) or 0.5 μM dexamethasone (B,D,F), and stained for immunofluorescence microscopy with anti-Man II (A,B,C,D), anti-β-COP (E,F), or anti-protein disulfide isomerase (PDI) (G,H) antibodies. Note the distinctive GC collapse in N-Ras-transformed cells (D,F). Bar, 10 μm.

To further examine the status of the GC, conventional electron microscopy was performed. The GC stack of transformed KT8 cells was fragmented but retained attached mini-cisternae (Fig. 4B, arrows). No ultrastructural changes were observed in other organelles such as the ER, lysosomes or mitochondria. Stereological analysis (Table 1) showed that the surface density of Golgi cisternae was significantly increased, without changes in the volume of Golgi cisternae. In addition, there was no change in the density volume of the GC relative to the cytoplasm. Therefore, the increase in membrane surface of the Golgi cisternae in transformed KT8 cells can be attributed to their fragmentation.

The Golgi complex collapse induced by N-Ras is associated with the disassembly of actin microfilaments

Double-label confocal immunofluorescence experiments were performed to analyze the GC in parallel with the status of microtubules (Fig. 5) and actin microfilaments (Fig. 6). Dexamethasone-induced KT8 cells showed a collapsed GC against a background of intact microtubules (Fig. 5B). On the other hand, nocodazole treatment resulted in microtubular network disruption and dispersion of GC fragments both in control (Fig. 5C) and in transformed KT8 cells (Fig. 5D). In addition, no differences in control versus transformed cells were observed when a time-course of microtubule depolymerization by cold treatment was performed (not shown). Therefore, the GC morphological alteration induced by N-Ras requires an intact microtubular network.

In contrast to the stability of the microtubular network, transformed KT8 cells showed a disruption of the actin cytoskeleton (Fig. 6A) concomitant with the appearance of the collapsed GC (Fig. 6B). The N-Ras-induced actin disassembly was quantitated by a fluorescent phalloidin binding assay, which reflects the amount of actin microfilaments, confirming that control KT8 cells contained significantly higher levels of F-actin than dexamethasone-induced KT8 cells (Fig. 7). The dependence of GC architecture on the actin cytoskeleton was further

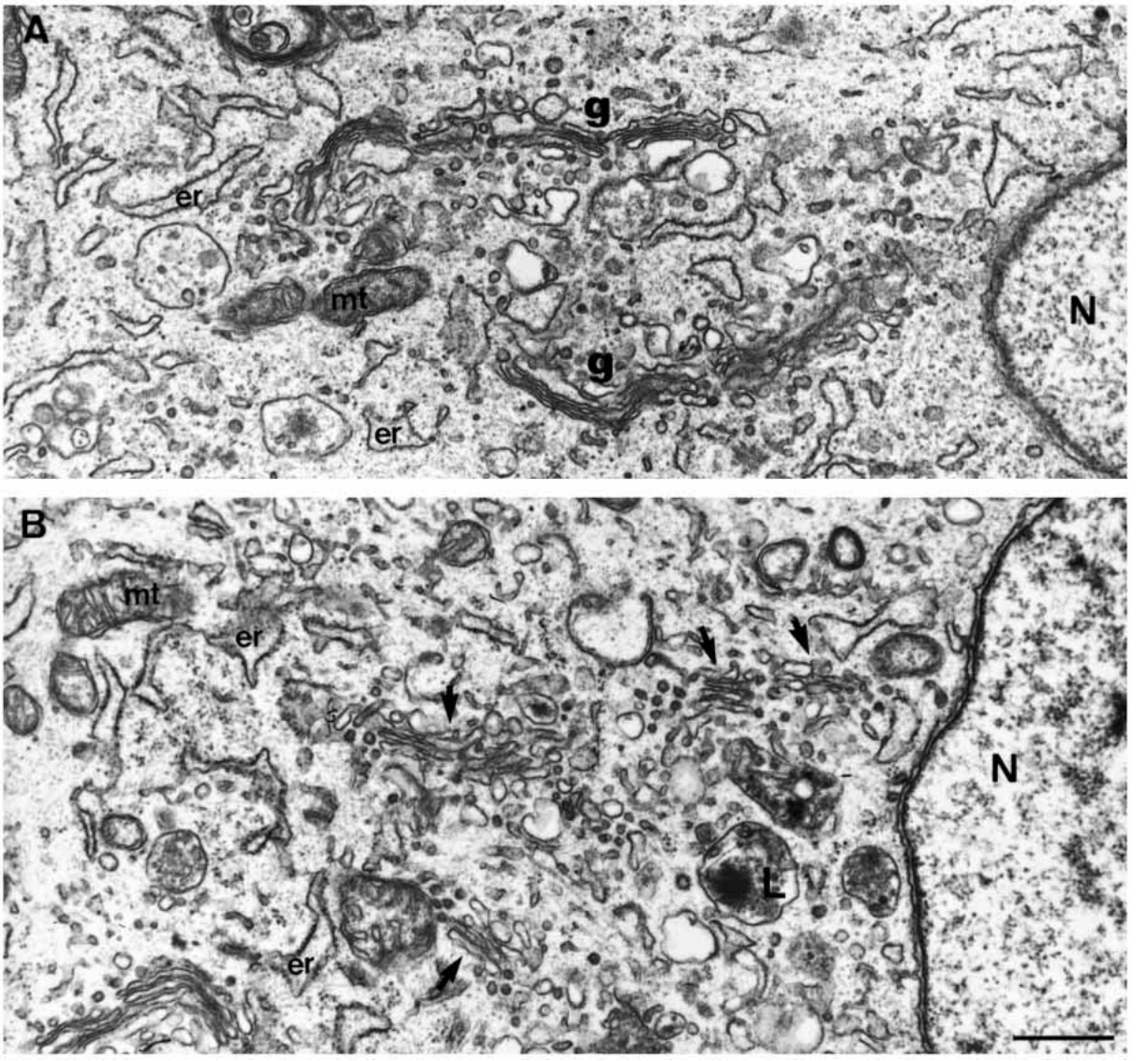

Fig. 4. Golgi complex (GC) fragmentation in N-Ras-transformed KT8 cells. At the EM level, the GC of control KT8 cells (A) appears as a continuous group of stacked cisternae. In N-Ras-transformed KT8 cells (B), Golgi stacks are fragmented, but maintain attached cisternae (arrows). G, Golgi complex; L, lysosome; N, nucleus; mt, mitochondria. Bar, 0.5 μm.

substantiated by treatment with the actin-disrupting drug cytochalasin D (cyD). This drug also produced a collapse of the GC in control KT8 cells, which appeared to be more severe than that induced by N-Ras-induced transformation (Fig. 6D). The N-Ras-induced disruption of actin microfilaments and the GC collapse were both reversed after withdrawal of dexamethasone (Fig. 8). Quantitation by the phalloidin binding assay showed that the recovery of the F-actin content (Fig. 8G) and the restoration of the GC morphology (Fig. 8C,E) followed similar kinetics. Thus, the reversal of the GC to its normal morphology is closely associated with the restitution of actin microfilaments, which appear before the cytochemical visualization of stress fibers. Altogether, these results indicate that N-Ras reversibly disrupts the actin cytoskeleton, and confirm our previous observations, utilizing actin-disrupting agents, that the morphology and subcellular localization of the GC is also controlled by actin microfilaments (Valderrama et al., 1998).

The phospholipase A_2 signal transduction pathway is involved in the Golgi complex alterations induced by N-Ras

We next performed experiments to determine which of the effectors and pathways known to be regulated by N-Ras could be involved in its effects on GC integrity. Phosphatidylinositide 3′-kinase (PI3K) is a downstream effector of the Ras protein (Kodaki et al., 1994; Rodríguez-Viciana et al., 1994) and is involved in the control of vesicular traffic (Brown et al., 1995; Davidson, 1995; De Camilli et al., 1996). When dexamethasone-induced KT8 cells were incubated with wortmannin at concentrations that specifically block PI3K activity (10-100 nM) (Stack et al., 1994), neither the collapse of the GC nor the actin disassembly were prevented (not shown). This result indicates

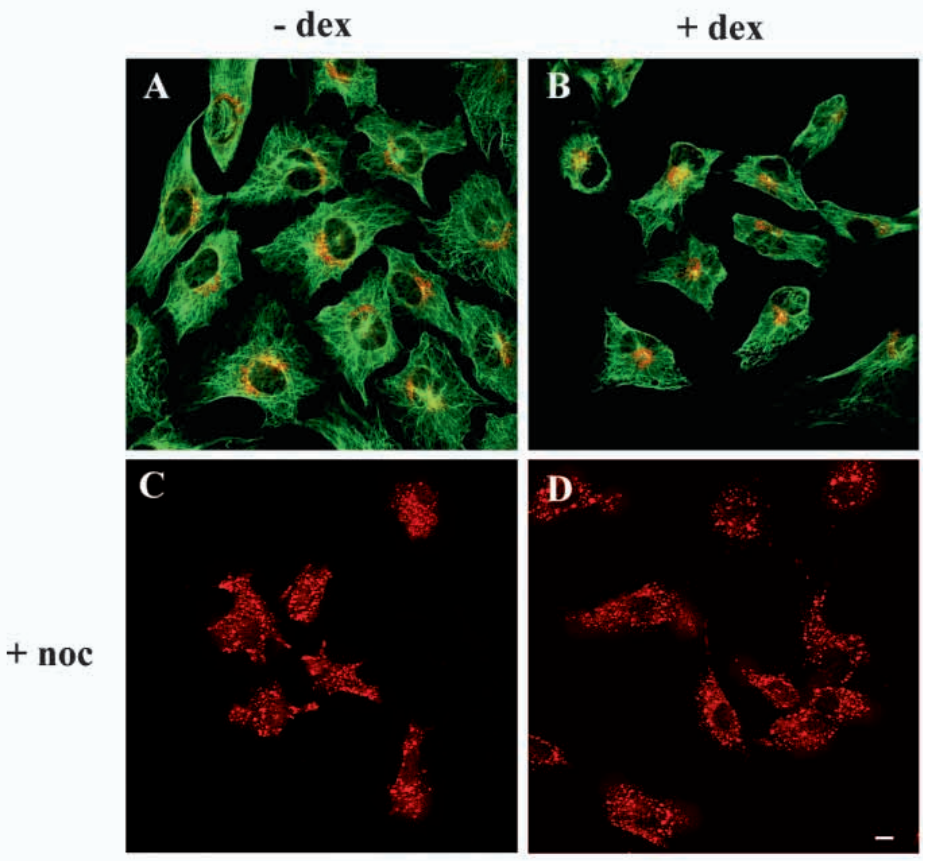

Fig. 5. The Golgi complex collapse induced by N-Ras requires an intact microtubular network. Double (A,B) or single (C,D) confocal immunofluorescence experiments in control (A,C) and dexamethasone-induced (B,D) KT8 cells stained with anti-Man II (A-D) and anti-tubulin (A,B) antibodies. Note that in dexamethasone-induced KT8 cells the microtubular cytoskeleton remains intact whilst the GC collapse occurs (B). When control (C) and dexamethasone-induced (D) KT8 cells were treated with the microtubule-disrupting agent nocodazole (noc), the GC appears, as expected, extensively fragmented and dispersed throughout the cytoplasm. Bar, 10 μm.

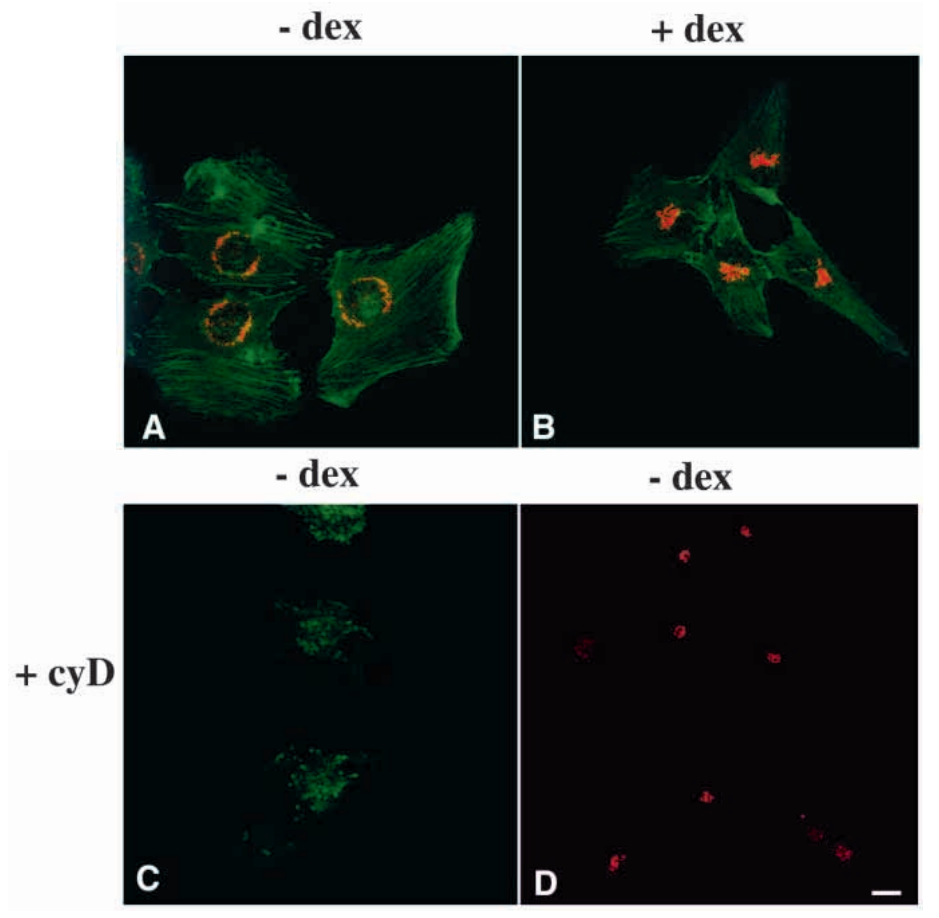

Fig. 6. The Golgi complex collapse induced by N-Ras is concomitant with the disassembly of actin microfilaments. Double (A,B) or single (C,D) confocal immunofluorescence experiments in control (A,C,D) or dexamethasone-induced (B) KT8 cells stained with anti-Man II (A,B,D) and anti-actin (C) antibodies or FITC-phalloidin (A,B). Dexamethasone-induced KT8 cells show the GC collapse and disassembly of the actin cytoskeleton (B). Treatment of control KT8 cells with cytochalasin D (cyD) (1 μM, 30 minutes) (C,D) produces a similar but more severe collapsed morphology of the GC (compare B with D). Bar, 10 μm.

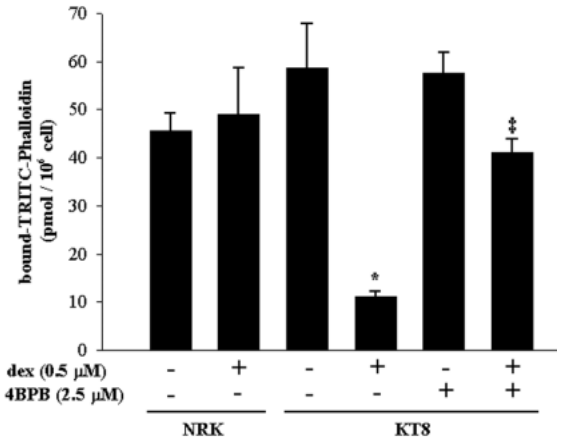

Fig. 7. N-Ras-induced disassembly of actin microfilaments is prevented by the PLA_2 inhibitor 4BPB. NRK and KT8 cells were incubated in the absence or presence of dexamethasone (16 hours) and/or 4BPB, and the content of F-actin was quantitated by the fluorescent phalloidin-binding assay. Data are the means ± s.e.m. from three independent experiments. Student's *t*-test demonstrates significant differences between (*) control and dexamethasone-induced KT8 cells ($P \leq 0.01$) and (‡) dexamethasone-induced KT8 cells without or with 4BPB pretreatment ($P \leq 0.05$).

that the GC and actin cytoskeleton alterations induced by N-Ras are not directly mediated by PI3K.

One of the major pathways governed by Ras proteins is the sequential phosphorylation of substrates in a cascade initiated by activation of the serine-threonine kinase Raf, followed by activation of MEK and MAP kinases. One of the substrates of MAP kinases is cytoplasmic PLA_2, which modulates the dynamics of the actin cytoskeleton through the production of derivatives of arachidonic acid (Lin et al., 1993; Peppelenbosch et al., 1993, 1995). In dexamethasone-induced KT8 cells, a significant increase in $cPLA_2$ activity is produced (from 11.3 ± 0.08 nmol/minute/ml to 15.5 ± 0.04 nmol/minute/ml, $P \leq 0.01$; means ± s.d. of three independent experiments). This activation was accompanied by an increase in the levels of the slower electrophoretic mobility species of $cPLA_2$ (Fig. 9), indicative of its phosphorylation by MAP kinase (Lin et al., 1993; Wijkander et al., 1995).

We thus tested the effect of the PLA_2 inhibitor 4-bromophenylacyl bromide (4BPB) (Peppelenbosch et al., 1993) in the N-Ras-induced effects on the GC architecture. The drug 4BPB significantly inhibited $cPLA_2$ activity (5.8 ± 0.1 nmol/minute/ml; $P \leq 0.01$) in dexamethasone-induced KT8 cells. Then, two different experimental approaches were followed: (1) dexamethasone and 4BPB were simultaneously added to KT8 cells in order to determine if 4BPB could prevent the N-Ras-induced collapse of the GC (Table 2); (2) dexamethasone-induced KT8 cells were incubated with 4BPB to determine if the GC collapse could be reverted (Table 3). Results showed that 4BPB partially inhibited and reverted the GC collapse induced by N-Ras. The F-actin content was also partially recovered (Fig. 7). Although it has been shown that 4BPB can affect microtubular integrity (Hargreaves et al., 1994), double labeling experiments with anti-Man II and anti-tubulin antibodies indicated that the microtubular network remained intact in the presence of 4BPB (not shown). Thus, these results

Table 2. Prevention of Golgi complex clustering by the $cPLA_2$ inhibitor 4BPB

	Cells with normal GC morphology (%)		
		+4BPB (μM)	
	–4BPB	1.25	2.5
Control cells	89.8±0.5	90.1±0.4	88.7±0.8
Induced cells	14.6±0.7	25.3±2.5	52.1±3.7

The percentage of KT8 cells with normal Golgi complex morphology (see Fig. 3C) was calculated from three separate experiments. Values are mean ± s.e.m. The total number of cells per experimental condition was 100.

KT8 cells were simultaneously incubated for 16 hours with dexamethasone (0.5 μM) and 4BPB (1.25 or 2.5 μM). Then, cells were fixed and stained for Golgi complex (ManII) and for actin microfilaments (TRITC-phalloidin) (see Fig. 7).

Table 3. Revertion of Golgi complex clustering by the $cPLA_2$ inhibitor 4BPB

	Cells with normal GC morphology (%)		
	–4BPB	+4BPB	
	2 days	1 day	2 days
Control cells	86.2±0.6	88.9±0.5	81.1±0.9
Induced cells	12.2±0.4	25.2±2.7	53.1±3.1

The percentage of KT8 cells with normal Golgi complex morphology (see Fig. 3C) was calculated from three separate experiments. Values are mean ± s.e.m. The total number of cells per experimental condition was 100.

KT8 cells were incubated with dexamethasone (0.5 μM) for 48 hours. Subsequently, 4BPB (2.5 μM) was added to the culture medium for 1 or 2 days. Thereafter, cells were fixed and stained for Golgi complex (ManII) and for actin microfilaments (TRITC-phalloidin).

indicate that PLA_2 is directly involved in the actin and the GC alterations produced by N-Ras-induced transformation.

N-Ras-induced transformation does not lead to aberrant glycosylation but increases the constitutive protein transport to the cell surface

We next analyzed if the conspicuous morphological changes in the GC were accompanied by functional alterations associated with this organelle, such as protein glycosylation and transport. It has been reported that transforming proteins alter the composition of cell surface carbohydrates (Santer et al., 1984; Collard et al., 1985). Increased β1,6 branching and sialic acid content in activated Ha-Ras transfection were previously observed (Bolscher et al., 1986; Dennis, 1991). It is also known that diverse lectins bind specifically to glycan structures of the cell surface and kill the cells in culture. Thus, the sensitivity of KT8 cells to lectin-mediated cytotoxicity was measured (Stanley, 1983). Dexamethasone-induced KT8 cells did not show any increase in the sensitivity to L-PHA (which specifically binds to oligosaccharides containing β1,6 branching) or WGA (which binds sialic acid) (not shown). In addition, we used the VSV-G protein as a reporter molecule that can reflect modifications in protein glycans (Bolscher et al., 1986). Analysis by two-dimensional SDS-PAGE of the VSV-G glycoprotein in KT8 cells revealed that N-Ras-induced transformation did not produce any quantitative changes in the multiple spots that reflect the different glycosylated isoforms containing sialic acid residues (not shown).

We next investigated whether the secretory movement of

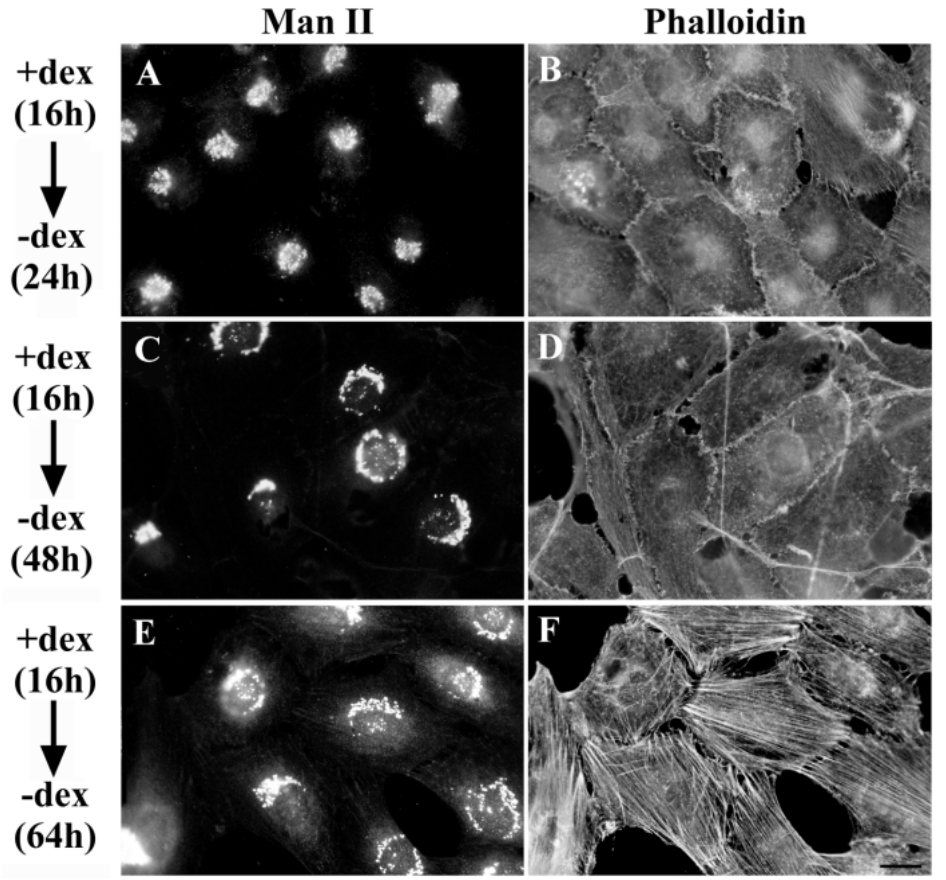

Fig. 8. Reversion of the N-Ras-induced Golgi complex collapse parallels recovery of F-actin content and precedes the visual appearance of stress fibers. After 24 hours (A,B), 48 hours (C,D) and 64 hours (E,F) of removal of dexamethasone (dex) (0.5 μM, 16 hours) from the culture medium, KT8 cells were double-labeled with anti-Man II antibodies (A,C,E) and TRITC-phalloidin (B,D,F). 24 hours after removal of dexamethasone, the GC remains collapsed (A) with disrupted actin microfilaments (B). 48 hours after removal of dexamethasone, the GC regains its normal morphology and subcellular arrangement in the majority of the cells (C), whereas actin microfilaments appear disassembled (D). 64 hours after removal of the inducer, the GC shows a normal appearance in all cells (E) and stress fibers are visible (F). (G) Measurement of the F-actin content by the fluorescent phalloidin-binding assay at different times after the dexamethasone withdrawal. ▲, the F-actin content in control KT8 cells. Results are the means ± s.d. of three independent experiments. Bar, 10 μm.

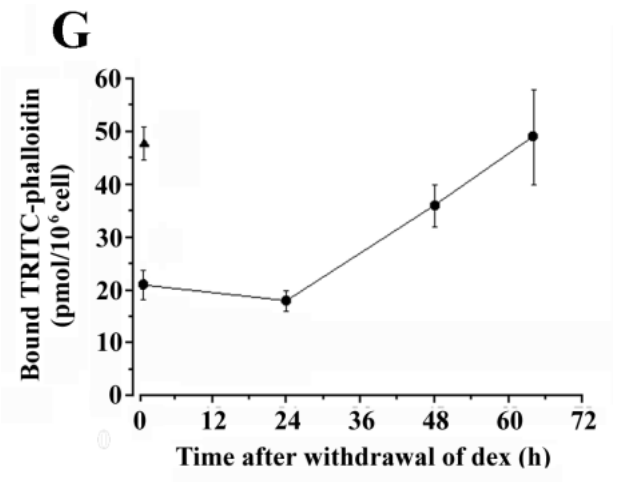

proteins was altered by N-Ras transformation. For this, we analyzed the ER-to-plasma membrane, ER-to-Golgi, and TGN-to-plasma membrane trafficking steps. When we studied the ER-to-plasma membrane transport of the VSV-G glycoprotein (Fig. 10A) and secretory proteins (Fig. 10B), dexamethasone-induced KT8 cells showed an increased transport both in the rate and extent of VSV-G (Fig. 10A) and secretory proteins to cell surface (Fig. 10B). Half of the secretory protein release was already achieved after 12 minutes in dexamethasone-induced KT8 cells relative to 24 minutes in control KT8 cells (Fig. 10B). Importantly, 4BPB (2.5 μM) inhibited the N-Ras-induced increase in the constitutive protein secretion (Fig. 10B). Treatment of NRK cells with dexamethasone did not alter protein secretion levels (not shown). Consequently, we next analyzed the sequential membrane transport step(s) altered by N-Ras-induced transformation. Thus, we assayed ER-to-Golgi, and TGN-to-plasma membrane transports. As shown in Fig. 11, dexamethasone-induced KT8 cells did not show any difference in the processing of newly synthesized VSV-G glycoprotein to the Endo H-resistant form. Moreover, the treatment with 4BPB (Fig. 11) or cyD (not shown) did not produce any alteration either in transformed or control KT8 cells. These results argue that transport from the ER-to-GC is not altered by N-Ras, despite any other effects of 4BPB, and confirm that there is no involvement of actin microfilaments in the ER-to-Golgi membrane dynamics (Valderrama et al., 1998). Finally, we studied the TGN-to-plasma membrane transport (Fig. 12). After an incubation at 20°C to block material in the TGN, VSV-G transported to the cell membrane was analyzed. In particular, control and dexamethasone-induced KT8 cells were infected for 3 hours at the restrictive temperature and subsequently incubated for 1 hour at 20°C. Under these experimental conditions, VSV-G accumulates in the TGN (Griffiths and Simons, 1986). Cells were subsequently transferred to 32°C in the absence or presence of 4BPB or cyD, and based on fluorescence-activated cell sorting (FACS) analysis using an antibody specific for the VSV-G protein ectodomain, VSV-G was transported to the plasma membrane (Fabbri et al., 1994). VSV-G was faster and more extensively transported in N-Ras-transformed KT8 cells. The presence of

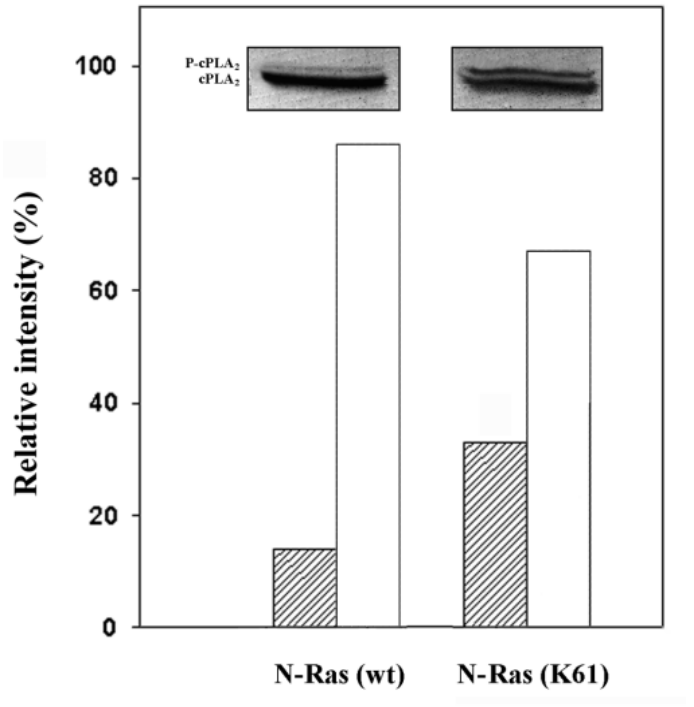

Fig. 9. N-Ras transformation stimulates the activation of PLA_2 activity. (Inset) Western blot analysis with anti-$cPLA_2$ antibodies in control (left) and dexamethasone-induced (16 hours) (right) KT8 cells. The slower migrating band corresponds to phosphorylated $cPLA_2$ ($P\text{-}cPLA_2$). Bands were quantitated by densitometric scanning and expressed as a percentage of total protein distributed in each band. Open columns, $cPLA_2$; hatched columns, $P\text{-}cPLA_2$. Note the increase in the percentage of the phosphorylated $cPLA_2$ form in N-Ras-transformed cells. Single representative data from two independent experiments are shown.

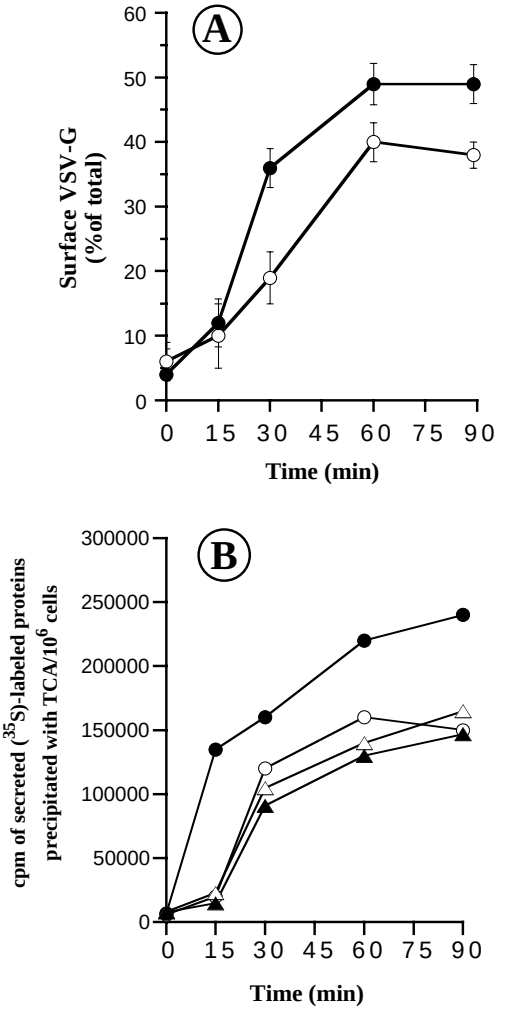

Fig. 10. The increase in the constitutive protein transport from the ER to the cell surface induced by N-Ras is inhibited by 4BPB. (A) Control (open circles) and dexamethasone-induced (16 hours) (filled circles) KT8 cells infected with VSV and labeled with [^{35}S]methionine were blocked at 40°C to accumulate material in the ER. Cells were chased at 32°C for the indicated times. Biotinylated cell surface proteins were precipitated with streptavidin-agarose and quantitated. Note that in N-Ras-transformed cells, the rate and extent of VSV-G transport to the plasma membrane is increased. Values are the means ± s.d. of three independent experiments. (B) KT8 cells were incubated for 16 hours in the absence (open symbols) or presence (filled symbols) of dexamethasone with (triangles) or without (circles) 4BPB (2.5 μM). KT8 cells were then pulse-labeled and chased for different times, as indicated. Total proteins released into the culture medium were precipitated with TCA, resuspended, and counted as described in Materials and methods. N-Ras induces an increase in the constitutive release of secretory proteins that is inhibited when KT8 cells are incubated with the PLA_2 inhibitor 4BPB. Values are the means of duplicate measurements.

4BPB or cyD in control KT8 cells did not produce significant alterations in the transport of VSV-G to the cell membrane. However, 4BPB prevented the N-Ras-induced increase in VSV-G transport from TGN-to-plama membrane. These results indicate that N-Ras-induced transformation stimulates TGN-to-plasma membrane but not ER-to-Golgi transport.

DISCUSSION

In this study, we show that N-Ras-induced transformation produces GC collapse and stack fragmentation, and an increase in protein transport from the TGN to the cell surface. In order to identify mediators of these effects we have focused our attention on the cytoskeleton and two major downstream effectors of Ras proteins, PI3K and PLA_2. The collapse of the GC is accompanied by the disassembly of actin microfilaments but not of microtubules (Prendergast and Gibbs, 1993; Dartsch et al., 1994). The observation that cyD also induced the collapse of the GC further supports the importance of the actin cytoskeleton in the maintenance of the normal arrangement of the GC in the cell (Valderrama et al., 1998). The block of expression of oncogenic N-*ras* by removal of dexamethasone allowed the GC to return to its normal morphology and subcellular arrangement, in parallel with the recovery of the F-actin content. Thus, our results indicate that the disruption of the GC morphology correlates with the disruption of filamentous actin. Recovery of F-actin to levels sufficient for the reconstitution of the GC architecture preceded the appearance of visible actin stress fibers. Thus, the GC is most likely linked to actin microfilaments that do not form part of

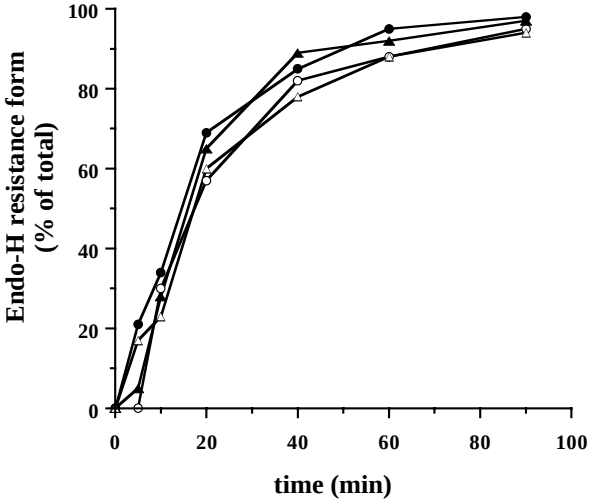

Fig. 11. The VSV-G glycoprotein transport from the ER to the Golgi complex is not altered by N-Ras. KT8 cells were infected with the VSV ts045 temperature-sensitive mutant virus, labeled with [^{35}S]methionine at 40°C and chased at 32°C at different times, as indicated, to study the ER-to-Golgi transport by acquisition of the Endo-H resistant form of the VSV-G glycoprotein. Note that no change in the kinetics of the arrival of G-protein to the GC is observed in either control (open circles) or dexamethasone-induced (filled circles) KT8 cells. Pretreatment with 4BPB (2.5 μM, 16 hours) in control (open triangles) and dexamethasone-induced (filled triangles) KT8 cells does not produce any significant changes in ER-to-Golgi transport of VSV-G.

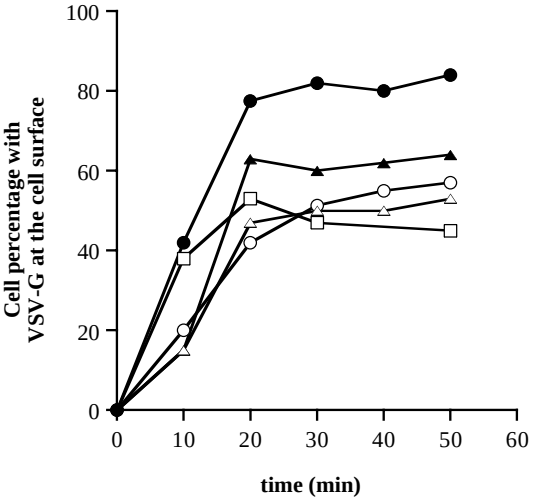

Fig. 12. The transport of VSV-G from the TGN to the plasma membrane is increased by N-Ras. Control (open circles) and dexamethasone-induced (filled circles) KT8 cells were infected with VSV for 3 hours at the restrictive temperature (40°C) and then incubated at 20°C for 60 minutes to accumulate VSV-G in the TGN and, consequently, to block transport to the cell surface. To detect VSV-G on the plasma membrane, cells were washed in ice-cold PBS containing 1% mouse serum and stained with an antibody recognizing the extracytoplasmic domain of VSV-G, followed by an FITC-conjugated goat anti-rabbit second antibody. The fraction of cells containing VSV-G on the cell surface was measured by FACS analysis. Note that dexamethasone-induced KT8 cells show an increase in TGN-to-plasma membrane transport (filled circles). This increase is inhibited by pretreatment with 4BPB (2.5 μM, 16 hours) (filled triangles). Moreover, the treatment with cyD (1 μM) in control KT8 cells (open squares) does not produce any significant change in the rate of VSV-G transported to the cell surface.

stress fibers. In fact, we have also observed (F. Valderrama, T. Babià, A. Luna, J. W. Kok and G. Egea, unpublished) that when NRK cells are incubated or microinjected with *Botulinum toxin* C3, a toxin that specifically inactivates the stress fiber formation-controlling small GTPase protein Rho (Ridley and Hall, 1992), the actin stress fibers are disrupted, but the interconnected reticular GC morphology stained with anti-Man II antibodies remained unaltered. It is also possible that, in induced KT8 cells, the actin cytoskeleton specifically linked to the GC is disassembled in the first instance, followed then by the actin stress fibers. Upon removal of the inducer, the reconstitution of the actin cytoskeleton would follow the same order. Consequently, the GC morphology recovers before the formation of stress fibers. The correlation between actin disassembly and the GC collapse is not exclusive of N-Ras-induced transformation. In K-Ras transformed (KiKi) rat thyroid cells, the GC is also tightly collapsed and the internal, but not the cortical, actin cytoskeleton is disrupted (I. Ayala, M. G. Silletta, D. Corda and G. Egea, unpublished results). These observations indicate that actin microfilaments are needed to exert a 'pushing force' on the GC to maintain its morphology and cytological localization, and that the resulting clustering of the GC could simply reflect an equilibrium between the inward and outward membrane movements governed only by the microtubular motors. Thus, the actin and microtubular cytoskeletons are essential and complementary webs that maintain the architecture and the cytological positioning of the GC.

Induction of the activated N-Ras oncoprotein caused a sustained and simultaneous translocation of the MAP kinase ERK2 to the nucleus and to the cell periphery, a hallmark of MAP kinase activation (Chen et al., 1992; González et al., 1993). MAP kinases phosphorylate and activate $cPLA_2$ (Lin et al., 1993), which in turn causes disruption of F-actin containing stress fibers (Peppelenbosch et al., 1993, 1995). Since the N-Ras-induced disruption of actin microfilaments and alterations in the GC were significantly prevented by 4BPB, our observations suggest a sequential link between the expression of plasma membrane-associated activated N-Ras, activation of the Raf kinase/MAP kinase pathway, an enzymatic activation of $cPLA_2$ and, finally, the alteration in the actin cytoskeleton and GC integrity. However, inhibition of PLA_2 does not completely prevent these alterations, leaving the possibility that activation of other small GTP-binding proteins or other downstream effectors of Ras are involved in the regulation of the GC structure and/or actin organization. Recently, it has been reported that Golgi fragmentation occurring during mitosis depends on activation of MEK1 (Acharya et al., 1998), a direct downstream effector of the Ras/Raf/MAPK signalling pathway. Interestingly, N-Ras-transformed and mitotic cells share the signalling activation of MEK1, although in N-Ras-transformed KT8 cells, GC fragments remain juxtanuclearly located, whereas in permeabilized NRK cells incubated with mitotic extracts, GC fragments are dispersed throughout the cytoplasm (Acharya et al., 1998). It is therefore possible that in N-Ras-transformed

cells, the concomitant disassembly of actin microfilaments impairs the cytoplasmic dispersion of GC fragments.

Most probably, the GC collapse and stack fragmentation are coincidental but independently generated phenomena. This hypothesis is based on the observation that in cyD-treated cells, the GC was tightly collapsed, but the stacks of cisternae appeared swollen and not fragmented (Valderrama et al., 1998). A possible explanation would be that the reticular morphology of the GC and its cytological positioning are maintained by the actin cytoskeleton, whereas the integrity of the Golgi stack is regulated by an intracellular PLA_2 activity that could produce tubulation (de Figueiredo et al., 1998) and/or fragmentation by altering membrane lipid composition. Previous reports have shown the presence of an endogenous Golgi phospholipase A activity (Moreau and Morre, 1991) correlated with an in vitro ER-to-Golgi and intra-Golgi transport (Slomiany et al., 1992; Tagaya et al., 1993).

GC morphological alterations induced by N-Ras lead to a significant increase in the constitutive protein transport from the TGN to the cell surface. The observation that control KT8 cells treated with cyD do not alter this protein transport indicates that the integrity of actin microfilaments is not essential for the constitutive secretory transport. Moreover, preliminary results in other cell lines show that cyD and latrunculin B do not significantly alter constitutive secretion (I. Ayala, A. Luna, M. Baldassarre, A. Luini, R. Buccione and G. Egea, unpublished results). However, the blocking effect of 4BPB on the increased delivery of proteins to the cell surface suggests a functional role of an intracellular PLA_2 in the constitutive protein transport from the TGN to the cell surface. However, besides the TGN-to-plasma membrane transport increase induced by N-Ras, an intra-Golgi alteration is also posible since previous results have also shown a correlation between PLA_2 acitvity and in vitro intra-Golgi transport.

Also of interest is that N-Ras did not induce changes either in the VSV-G protein glycosylation or the cell surface content of sialic acid and oligosaccharides containing β1,6 branching. This appears to be in contrast to the results previously described with Ha-Ras (Bolscher et al., 1986). Substantial differences in the two models of transformation and/or Ras oncoprotein involved might account for these discrepancies. In particular, the NIH3T3 model displays a morphological transformation only after two passages in the presence of the inducer dexamethasone. Furthermore, in this NIH3T3 model the Ras protein is observed only after 20 hours of induction, and described glycosylation alterations in the VSV-G protein were a late effect, being detected only 36 hours after the addition of dexamethasone. Even considering that activation of a given signalling pathway can produce different responses in different cells, a further extrapolation of our observations leads to the conclusion that alterations in glycosylation patterns and vesicular transport found in transformed cells may not be solely a direct consequence of the expression of activated Ras proteins.

Our sincere thanks to Dr Roberto Buccione, Dr Alberto Luini and Dr Vivek Malhotra for reading of the manuscript, Dr Antonio García de Herreros for useful suggestions, Maite Muñoz for skilful technical assistance, Dr Pablo Engel for help and advice with the FACS, Susana Castel (Serveis Científico-Tècnics, Universitat de Barcelona) for assistance with confocal microscopy, and Dr C. P. Berrie for editorial assistance. We also thank Dr A. Velasco (Universidad de Sevilla, Spain), Dr G. Banting (Univeristy of Bristol, UK), Dr K. Simons (EMBL, Heidelberg, Germany), Dr J. G. Castaño (UAM, Madrid, Spain) and the late Dr T. Kreis (University of Geneva, Switzerland) for generous gifts of antibodies. T.B. is the recipient of a postdoctoral fellowship from CIRIT (Catalunya, Spain). F.V. and I.A. are predoctoral fellows from the Universitat de Barcelona and Ministerio de Educación y Ciencia, respectively. J.W.K. is supported by the Royal Netherlands Academy of Arts and Sciences. This work is supported by grants to G.E. (SAF 97/0016 and TeleMarató de Catalunya TV3) and to T.M.T. (DGICYT PB-092-0506-CO2-01 and from the Fundación Científica de la Associación Española contra el Cáncer and the Fundación Ramón Areces).

REFERENCES

Alcalde, J., Egea, G. and Sandoval, I. V. (1994). gp74 a membrane glycoprotein on the *cis*-Golgi network that cycles through the endoplasmic reticulum and intermediate compartment. *J. Cell Biol.* **124**, 649-665.

Acharya, U., Mallabiabarrena, A., Acharya, J. K. and Malhotra, V. (1998). Signaling via Mitogen-activated protein kinase kinase (MEK1) is required for Golgi fragmentation during mitosis. *Cell* **92**, 183-192.

Berger, E. G. and Roth, J. (1997). *The Golgi Apparatus* (ed. E. G. Berger and J. Roth). Birkhäuser Verlag, Basel.

Bar-Sagi, D. and Feramisco, J. R. (1986). Induction of membrane ruffling and fluid-phase pinocytosis in quiescent fibroblasts by ras proteins. *Science* **233**, 1061-1068.

Bolscher, J. G., Schallier, D. C., Smets, L. A., van Rooy, H., Collard, J. G. and Bruyneel, E. A. (1986). Effect of cancer-related and drug-induced alterations in surface carbohydrates on the invasive capacity of mouse and rat cells. *Cancer Res.* **46**, 4080-4086.

Bolscher, J. G., Bijl, M. M. W. v. d., Neefjes, J. J., Hall, A., Smets, L. A. and Ploegh, H. L. (1988). Ras (proto)oncogene induces N-linked carbohydrate modification: temporal relationship with induction of invasive potential. *EMBO J.* **7**, 3361-3368.

Bomsel, M. and Mostov, K. (1992). Role of heterotrimeric G proteins in membrane traffic. *Mol. Biol. Cell* **3**, 1317-1328.

Bond, V. C. and Wold, B. (1987). Poly-L-ornithine-mediated transformation of mammalian cells. *Mol. Cell Biol.* **7**, 2286-2293.

Bos, J. L. (1989). Ras oncogenes in human cancer: a review. *Cancer Res.* **49**, 4682-4689.

Bourne, H., Sanders, D. A. and McCormick (1990). The GTPase superfamily: a conserved switch for diverse cell functions. *Nature* **348**, 125-132.

Brown, W. J., de Wald, D. B., Emr, S. D., Putner, H. and Balch, W. E. (1995). Role of phosphatidylinositol-3-kinase in the sorting and transport of newly synthesized lysosomal enzymes in mammalian cells. *J. Cell Biol.* **130**, 781-796.

Buccione R, Bannykch S., Santone, I., Baldassarre, M., Facchiano F., Bozzi, Y., Di Tullio, G., Mironov, A., Luini, A. and De Matteis, A. (1996). Regulation of constitutive exocytic transport by membrane receptors. *J. Biol. Chem.* **271**, 3523-3533.

Chen, R. H., Sarnecki, C. and Blenis, J. (1992). Nuclear localization and regulation of erk- and rsk-encoded protein kinases. *Mol. Cell Biol.* **12**, 915-927.

Chomczynski, P. and Sacchi, N. (1987). Single-step method of RNA isolation by acid guanidinium. *Anal. Biochem.* **162**, 156-159.

Collard, J. G., van Beek, W. P., Janssen, J. W. G. and Schijven, J. F. (1985). Transfection by human oncogenes: concomitant induction of tumorigenicity and tumor-associated membrane alterations. *Int. J. Cancer* **25**, 207-213.

Dartsch, P. C., Ritter, D., Häussinger, D. and Lang, F. (1994). Cytoskeletal reorganization in NIH 3T3 fibroblasts expressing the ras oncogene. *Eur. J. Cell Biol.* **63**, 316-325.

Davidson, D. (1995). Wortmannin causes mistargeting of procathepsin D. Evidence for the involvement of a phosphatidylinositol 3-kinase in vesicular transport ot lysosomes. *J. Cell Biol.* **130**, 797-805.

De Camilli, P., Emr, S. D., McPherson, P. S. and Novick, P. (1996). Phosphoinositides as regulators in membrane traffic. *Science* **271**, 1533-1539.

De Figueiredo, P., Drecktrach, D., Katzenellenbogen, J. A., Strang, M. and Brown W. J. (1998). Evidence that phospholipase A2 activity is required for Golgi complex and trans Golgi network membrane tubulation. *Proc. Nat. Acad. Sci. USA* **95**, 8642-8647.

De Matteis, M. A., Santini, G., Kahn, R. A., Di Tullio, G. and Luini, A.

(1993). Receptor and protein kinase C-mediated regulation of ARF binding to the Golgi complex. *Nature* **364**, 818-821.

De Hoop, M. and Cid-Arregui, A. (1996). Use of Flowl Plague Stomatitis and Semliki Forest Viruses to study the mechanisms of neuronal membrane polarity. In *Protocols for Gene Transfer in Neuroscience: Towards Gene Terapy of Neurological Disorders* (ed. P. R. Lowenstein and L. W. Enquist), pp. 65-77. John Wiley and Sons Ltd.

Denker, S. P., McCaffery, J. M., Palade, G. E., Insel, P. A. and Farquhar, M. G. (1996). Differential distribution of α subunits and βγ subunits of heterotrimeric G proteins on Golgi membranes of the exocrine pancreas. *J. Cell Biol.* **133**, 1027-1040.

Dennis, J. W. (1991). N-linked oligosaccharide processing and tumor cell biology. *Sem. Cancer Biol*. **2**, 411-420.

Fabbri, M., Bannykh, S. and Balch, W. E. (1994). Export of protein from the endoplasmic reticulum is regulated by a diacylglycerol/phorbol ester binding protein. *J. Biol. Chem.* **269**, 26848-26857.

Farquhar, M. G. and Palade, G. E. (1998). The Golgi apparatus: 100 years of progress and controversy. *Trends Cell Biol*. **8**, 2-10.

Gelperin, D., Weigle, J., Nelson, K., Roseboom, P., Iri, K., Matsumoto, K. and Lemmon, S. (1995). 14-3-3 proteins: Potential roles in vesicular transport and ras signaling in *Saccharomyces cerevisiase*. *Proc. Nat. Acad. Sci. USA* **92**, 11539-11543.

Griffiths, G. and Simons, K. (1986). The trans-Golgi network: sorting at the exit site of the Golgi complex. *Science* **234**, 438-443.

González, F. A., Seth, A., Raden, D. L., Bowman, D. S., Fay, F. S. and Davis, R. J. (1993). Serum-induced translocation of mitogen-activated protein kinase to the cell surface ruffling membrane and the nucleus. *J. Cell Biol*. **122**, 1089-1101.

Goodnight, J. A., Mischak, H., Kolch, W. and Mushinski, J. F. (1995). Immunocytochemical localization of eight protein kinase C isozymes overexpressed in NIH 3T3 fibroblasts. Isoform-specific association with microfilaments, Golgi, endoplasmic reticulum and nuclear and cell membranes. *J. Biol. Chem*. **270**, 9991-10001.

Guerrero, I., Wong, H., Pellicer, A. and Burstein, D. E. (1986). Activated N-ras gene induces neuronal differentiation of PC12 rat pheochromocytoma cells. *J. Cell Physiol*. **129**, 71-76.

Hakomori, S. I. (1989). Aberrant glycosylation in tumors and tumor-associated carbohydrate antigens. *Adv. Cancer Res.* **52**, 257-331.

Hall, A. (1990). The cellular function of small GTP-binding proteins. *Science* **249**, 635-640.

Hargreaves, A. J., Glaxier, A. P., Flaskos, J., Mullins, F. H. and McLean, G. (1994). The disruption of brain microtubules in vitro by the phospholipase inhibitor p-bromophenacylbromide. *Biochem. Pharmacol.* **47**, 1137-1143.

Kodaki, T., Woscholski, R., Hallberg, B., Rodríguez-Viciana, P., Downward, J. and Parker, P. (1994). The activation of phosphatidylinositol 3-kinase by Ras. *Curr. Biol*. **4**, 494-499.

Ktistakis, N. T., Brown, H. A., Sternweis, P. C. and Roth, M. G. (1995). Phospholipase D is present on Golgi-enriched membranes and its activation by ADP ribosylation factor is sensitive to brefeldin A. *Proc. Nat. Acad. Sci. USA* **92**, 4952-4956.

Lang, F., Ritter, M., Woll, E., Heiss, H., Häussinger, D., Hoflacher, J., Marly, K. and Grunicke, H. (1992). Altered cell volume regulation in *ras* oncogene expressing NIH fibroblasts. *Eur. J. Physiol.* **420**, 424-427.

Leyte, A., Barr, F. A., Kehenbach, R. H. and Huttner, W. B. (1992). Multiple trimeric G-proteins on the trans-Golgi network exert stimulatory and inhibitory effects on secretory vesicle formation. *EMBO J*. **11**, 4795-47804.

Lin, L. L., Wartmann, M., Lin, A. Y., Knopf, J. L., Seth, A. and Davis, R. J. (1993). cPLA$_2$ is phosphorylated and activated by MAP kinase. *Cell* **72**, 269-278.

Machesky, L. M. and Hall, A. (1996). Rho: a connection between membrane receptor signalling and the cytoskeleton. *Trends Cell Biol.* **6**, 304-310.

Melançon, P., Glick, B. S., Malhorta, V., Weidman, P. J., Serafini, T., Gleason, M. L., Orci, L. and Rothman, J. E. (1987). Involvement of GTP-binding 'G' proteins in transport through the Golgi stack. *Cell* **51**, 1053-1062.

Moreau, P. and Morre, D. J. (1991). Cell-free transfer of membrane lipids. Evidence for lipid processing. *J. Biol. Chem.* **266**, 4329-4333.

Muñiz, M., Alonso, M., Hidalgo, J. and Velasco, A. (1996). A regulatory role for cAMP-dependent protein kinase in protein traffic along the exocytic route. *J. Biol. Chem.* **271**, 30935-30941.

Peppelenbosch, M. P., Tertoolen, L. G., Hage, W. J. and de Laat, S. W. (1993). Epidermal growth factor-induced actin remodeling is regulated by 5-lipoxygenase and cyclooxygenase products. *Cell* **74**, 565-575.

Peppelenbosch, M. P., Qiu, R. G., de Vries Smits, A. M., Tertoolen, L. G., de Laat, S. W., McCormick, F., Hall, A., Symons, M. H. and Bos, J. L. (1995). Rac mediates growth factor-induced arachidonic acid release. *Cell* **81**, 849-856.

Pfeffer, S. R. (1994). Rab GTPases: master regulators of membrane trafficking. *Curr. Opin. Cell Biol.* **6**, 522-526.

Pimplikar, S. W. and Simons, K. (1994). Activators of protein kinase A stimulate apical but not basolateral transport in epithelial Madin-Darby canine kidney cells. *J. Biol. Chem.* **269**, 19054-19059.

Prendergast, G. C. and Gibbs, J. C. (1993). Pathways of Ras function: connections of the actin cytoskeleton. *Adv. Cancer Res*. **62**, 19-64.

Prestle, J., Pfizenmaier, K., Brenner, J. and Johanner, F. J. (1996). Protein kinase C μ is located at the Golgi compartment. *J. Cell Biol.* **134**, 1401-1410.

Renau-Piqueras, J., Miragall, F., Guerri, C., Báguena-Cervellera, R. (1987). Prenatal exposure to alcohol alters the Golgi apparatus of newborn rat hepatocytes: a cytochemical study. *J. Histochem. Cytochem.* **35**, 221-228.

Ridley, A. J. and Hall, A. (1992). The small GTP-binding protein Rho regulates the assembly of focal adhesions and actin stress fibers in response to growth factors. *Cell* **70**, 389-399.

Rodríguez-Viciana, P., Warne, P. H., Dhand, R., Vanhaesebroeck, B., Gout, I., Fry, M. J., Waterfield, M. D. and Downward, J. (1994). Phosphatidylinositol-3-OH kinase as a direct target of Ras. *Nature* **370**, 527-532.

Santarén, J. F. and García-Bellido, A. (1990). High-resolution two-dimensional gel analysis of proteins in wing imaginal discs: a data base of Drosophila. *Exp. Cell Res*. **189**, 169-176.

Santer, U. V., Gilbert, F. and Glick, M. C. (1984). Change in glycosylation of membrane glycoproteins after transfection of NIH 3T3 with human tumor DNA. *Cancer Res*. **44**, 3730-3735.

Simon, J. P., Ivanon, I. E., Adesnik, M. and Sabatini, D. D. (1996). The production of post-Golgi vesicles requires a protein kinase C-like molecule, but not its phosphorylating activity. *J. Cell Biol.* **135**, 355-370.

Slomiany, A., Grzelinska, E., Kasinathan, Ch., Yamaki, K-I., Palecz, D. and Slomiany, B. L. (1992). Function of intracellular phospholipase A$_2$ in vectorial transport of apoproteins from ER to Golgi. *Int. J. Biochem.* **24**, 1397-1406.

Stack, J. H. and Emr, S. D. (1994). Vps34p required for yeast vacuolar protein sorting is a multiple specificity kinase that exhibits both protein kinase and phosphatidylinositol-specific PI 3-kinase activities. *J. Biol. Chem.* **269**, 31552-61562.

Stanley, P. (1983). Selection of lectin-resistant mutants of animal cells. *Methods Enzymol*. **96**, 157-184.

Stow, J. L., de Almeida, J. B., Narula, N., Holtzman, E. J., Ercolani, L. and Ausiello, D. A. (1991). A heterotrimeric G protein, G$_{\alpha i3}$, on Golgi membranes regulates the secretion of a heparan sulfate proteoglycan in LLC-PK1 epithelial cells. *J. Cell Biol.* **114**, 1113-1124.

Symons, M. (1996). Rho family GTPases: The cytoskeleton and beyond. *Trends Biochem. Sci.* **21**, 178-181.

Tagaya, M., Henomatsu, N., Yoshimori, T., Yamamoto, A., Tashiro, Y. and Fukui, T. (1993). Correlation between phospholipase A$_2$ activity and intra-Golgi protein transport reconstituted in a cell-free system. *FEBS lett.* **324**, 201-204.

Valderrama, F., Babià, T., Ayala, I., Kok, J. W., Renau-Piqueras, J. and Egea G. (1998). Actin microfilaments are essential for the cytological positioning and morphology of the Golgi complex. *Eur. J. Cell Biol*. **76**, 9-17.

Weibel, E. R. (1979*). Practical Methods for Biological Morphometry*, Vol. 1. New York, Academic Press.

Wijkander, J., O'Flaherty, J. T., Nixon, A. B. and Wykle, R. L. (1995). 5-lipoxygenase products modulate the activity of the 85-Kda phospholipase A$_2$ in human neutrophils. *J. Biol. Chem.* **270**, 26543-26549.

Williams, M. (1977). Stereological Techniques. In *Practical Methods in Electron Microscopy*, Vol. 6 (ed. A. M. Glauert), pp. 1-82. Elsevier North Holland, Amsterdam.

Wöll, E., Weiss, H., Waldegger, S. and Lang, F. (1992). Effect of calcium channel antagonists on cell membrane potential oscillations and proliferation of cells expressing the *ras* oncogene. *Eur. J. Pharmacol*. **212**, 105-107.